

# Sol–Gel Derived Urea Cross-Linked Organically Modified Silicates. 1. Room Temperature Mid-Infrared Spectra

V. de Zea Bermudez,<sup>\*,†</sup> L. D. Carlos,<sup>‡</sup> and L. Alcácer<sup>§</sup>

*Secção de Química, Universidade de Trás-os-Montes e Alto Douro, Quinta de Prados, Apartado 202, 5001 Vila Real Codex, Portugal, Departamento de Física, Universidade de Aveiro, 3810 Aveiro, Portugal, Departamento de Engenharia Química, Instituto Superior Técnico, Rua Rovisco Pais, 1092 Lisboa Codex, Portugal*

*Received May 21, 1998. Revised Manuscript Received October 22, 1998*

Organic–inorganic hybrids prepared by the sol–gel process are investigated by infrared spectroscopy at room temperature. The matrix of the so-called *ureasils* is a silica network to which oligopolyoxyethylene chains are grafted by means of urea cross-links. The ureasils prepared—U(2000), U(900), and U(600)—are obtained by reacting three diamines (containing about 40.5, 15.5, and 8.5 oxyethylene units, respectively) with 3-isocyanatepropyltriethoxysilane. The mid-infrared spectra of the diamines are examined. The FTIR spectrum of U(2000) shows that the polyether chains of the parent diamine become less ordered upon incorporation into the inorganic backbone. The assignment of the absorption bands originating from the urea moieties in the ureasils is proposed. Spectroscopic data reveal that the number of oxyethylene units present affects dramatically the amide I and amide II bands and indicate that the N–H groups of the urea linkage are involved in hydrogen bonds of different strength. The existence of non-hydrogen-bonded urea groups and hydrogen-bonded urea–urea and urea–polyether associations is suggested. The formation of urea–urea structures is apparently favored in U(600), whereas the number of “free” carbonyl groups is greatest in U(2000).

## Introduction

Following Wright's<sup>1</sup> observations of ionically conductive complexes formed with poly(oxyethylene) (POE, (OCH<sub>2</sub>CH<sub>2</sub>)<sub>n</sub>) and salts, and the recognition by Armand et al.<sup>2</sup> that these polymer–salt complexes might work as suitable polymer electrolytes in all solid-state electrochemical devices, such as batteries, smart windows and sensors, these unique materials have been the focus of an intense investigation in the past two decades.<sup>3</sup>

The motion of ions in polymer matrices is a relatively new concept; the macromolecule itself acts as a solvent for a salt that becomes partially dissociated in the matrix, leading to electrolyte behavior. The development of polymer–salt complexes has paralleled that of host–guest chemistry, exemplified by crown ethers whose polymer analogues are open macromolecular host struc-

tures acting as polydentate ligands and containing preferably oxyethylene repeat units of the type OCH<sub>2</sub>–CH<sub>2</sub>, as it is the case in POE for which the space between two consecutive ether oxygens is optimal for coordination of metal cations. This hard polybasic molecule is able to solvate not only most alkali, alkaline and rare earth cations, but also transition metals, especially in their +2 state.

The interest for lanthanide cation-containing polyethers is quite recent.<sup>4–19</sup> New polymeric materials have

<sup>†</sup> Universidade de Trás-os-Montes e Alto Douro.

<sup>‡</sup> Universidade de Aveiro.

<sup>§</sup> Instituto Superior Técnico.

(1) Wright, P. V. *Br. Polym. J.* **1975**, *7*, 319.

(2) Armand, M.; Duclot, M. T.; Chabagno, J. M. *Proceedings of the Second International Meeting on Solid Electrolytes*, St. Andrews, Scotland, 1978.

(3) (a) *Polymer Electrolyte Reviews—1*; MacCallum, J. R., Vincent, C. A., Eds.; Elsevier: London, 1987. (b) *Electrochemical Science and Technology of Polymers 1*; Linford, R. G., Ed.; Elsevier: London, 1987. (c) *Polymer Electrolyte Reviews—2*; MacCallum, J. R., Vincent, C. A., Eds.; Elsevier: London, 1989. (d) *Proceedings of the 2nd International Symposium on Polymer Electrolytes*; Scrosati, B., Ed.; Elsevier Applied Science: London, 1990; (e) Gray, F. M. *Solid Polymer Electrolytes: fundamentals and technological applications*; VCH: New York, 1991. (f) *Electrochemical Science and Technology of Polymers 2*; Linford, R. G., Ed.; Elsevier: London, 1991.

(4) Huq, R.; Farrington, G. C. In *Proceedings of the 2nd International Symposium on Polymer Electrolytes*; Scrosati, B., Ed.; Elsevier Applied Science: London, 1990; p 281.

(5) Reis Machado, A. S.; Alcácer, L. In *Proceedings of the 2nd International Symposium on Polymer Electrolytes*; Scrosati, B., Ed.; Elsevier Applied Science: London, 1990; p 283.

(6) Twomey, C. J.; Chen, S. H. *J. Polym. Sci. B* **1991**, *29*, 859.

(7) Silva, C. J. R.; Smith, M. J. *Solid State Ionics* **1992**, *58*, 269.

(8) Smith, M. J. R.; Silva, C. J.; Silva, M. M. *Solid State Ionics* **1993**, *60*, 73.

(9) Petersen, G.; Torell, L. M.; Panero, S.; Scrosati, B.; Silva, C. J. R.; Smith, M. J. *Solid State Ionics* **1993**, *60*, 55.

(10) Silva, C. J. R.; Smith, M. J. *Electrochim. Acta* **1993**, *40*, 526.

(11) (a) Bernson, A.; Lindgren, J. *Solid State Ionics* **1993**, *60*, 31.

(b) Bernson, A.; Lindgren, J. *Solid State Ionics* **1993**, *60*, 37.

(12) (a) Carlos, L. D.; Assunção, M.; Abrantes, T. M.; Alcácer, L. *Solid State Ionics III*, Materials Research Society Proceedings; Nazri, G.-A., Tarascon, J.-M., Armand, M. B., Eds.; MRS: Pittsburgh, PA, 1993. (b) Carlos, L. D.; Videira, A. L. L. *Phys. Rev.* **1994**, *B49*, 11721.

(c) Carlos, L. D.; Videira, A. L. L. *J. Chem. Phys.* **1994**, *101*, 8827.

(13) Brodin, A.; Mattsson, B.; Torell, L. *J. Chem. Phys.* **1994**, *101*, 4621.

(14) (a) Carlos, L. D.; Videira, A. L. L.; Assunção, M.; Alcácer, L. *Electrochim. Acta* **1995**, *40*, 2143. (b) Carlos, L. D.; Assunção, M.; Alcácer, L. *J. Mater. Res.* **1995**, *10*, 202.

emerged in the past few years, and several groups have become involved worldwide in the research and development of luminescent polymeric systems for which elegant technological applications including optical devices, such as phosphors and solid-state lasers, may be foreseen.<sup>4,12-15,17,19</sup> The desirable characteristics of plastic materials, in particular their easy processability into films, are thus combined with the optical properties provided by the luminescent centers (mostly  $\text{Eu}^{3+}$  and  $\text{Nd}^{3+}$  cations). It was immediately recognized though that these materials, obtained by incorporating trivalent lanthanide salts into POE, are associated with two very severe drawbacks: (1) they tend to crystallize, a phenomenon that considerably reduces optical quality; (2) their highly hygroscopic nature makes handling in a glovebox compulsory. Another nuisance connected with the POE-based systems is the "salting-out effect" that prevails at high salt concentrations.

To overcome these inconveniences, we decided to change polymer architecture and to synthesize analogous luminescent polymers by using the sol-gel process. This chemical synthesis route is widely known as potentially attractive for the preparation of novel materials in many scientific fields. It relies on the great versatility of the silicon chemistry resulting from the remarkable stability of Si-O and Si-C bonds. Sol-gel offers substantial advantages over other techniques: (1) the precursors used are highly reactive, pure, and homogeneous; (2) the micro- and macrostructure of the host matrix may be controlled through the optimization of several parameters (e.g., water and/or alcohol content, temperature, pressure, type of catalyst, solvent); (3) the presence of the silica network provides simultaneously good mechanical resistance, extraordinary thermal stability, and amorphous character; (4) it is possible to graft organic groups into the inorganic backbone at low processing temperatures and to produce organic-inorganic hybrid materials designated as ormosils (organically modified silicates), ormolytes (organically modified silicate electrolytes), or ormocers (organically modified ceramics), depending on the final application; (5) elastomeric transparent monoliths of variable thickness, as well as powders, may be prepared. The sol-gel route proceeds through the hydrolysis and condensation of alkoxysilanes. After removal of the byproducts (water and alcohol), a rigid tridimensional network is formed. High-quality products may be obtained if special care is taken to prevent cracking during the drying procedure.

In the second half of 1997, several europium organic-inorganic silicate hybrids were first introduced and their spectral characteristics investigated.<sup>20,21</sup> Our group reported the synthesis and physical properties of a novel class of intensely luminescent Eu(III)-doped ormosils.<sup>20</sup> The sol-gel derived ormolytes proposed contain short,

highly solvating oxyethylene units grafted onto the inorganic network by means of urea bridges ( $-\text{NHC}(\text{=O})\text{NH}-$ ) and have been thus classed as ureasils (*ureasilicates*).<sup>22</sup>

The practical relevance of the europium-based ureasils is considerable. Apart from the fact that they are obtained as amorphous, slightly hygroscopic, and transparent monoliths, are thermally stable up to 250 °C, and exhibit an ionic conductivity of about  $10^{-5} \Omega^{-1} \text{cm}^{-1}$  at 30 °C, we have shown that these materials are multi-wavelength phosphors (i.e., white-light emitters), for the silica backbone itself is strongly luminescent.<sup>20</sup> Obviously, this optical feature is of the interest from the standpoint of application in technological luminescent devices. In past years the light emission of highly porous silicon layers has been extensively explored.<sup>23-29</sup> A great amount of effort has also been devoted to the study of light-emitting silicon-based materials with properties similar to those of porous silicon.<sup>29-31</sup> It is hoped that the luminescent properties of porous silicon and related materials will contribute in the near future to the growth of optical communication devices directly on silicon computer chips.<sup>28</sup>

The work presented here is the first of a series of two papers focused on the spectroscopic characterization of

(15) (a) Ohno, H.; Yoshihara, H. *Solid State Ionics* **1995**, *80*, 251. (b) Brodin, A.; Mattsson, B.; Torell, A.; Torell, L. M. *Electrochim Acta* **1995**, *40* (13-14), 2393.

(16) Gonçalves, A. R.; Silva, C. J. R.; Silva, M. M.; Smith, M. J. *Ionics* **1995**, *1*, 342.

(17) (a) Carlos, L. D.; Videira, A. L. L. *J. Chem. Phys.* **1996**, *105*, 8878. (b) Carlos, L. D. *Solid State Ionics* **1996**, *85*, 181.

(18) Bernson, A.; Lindgren, J. *Solid State Ionics* **1996**, *86-88*, 369.

(19) (a) Carlos, L. D.; Videira, A. L. L. *Chem. Phys. Lett.* **1997**, *57*, 264. (b) Ferry, A.; Furlani, M.; Franke, A.; Jacobsson, P.; Mellander, B.-E. *J. Chem. Phys.* **1998**, *109(7)*, 2921.

(20) (a) de Zea Bermudez, V.; Carlos, L. D.; Duarte, M. C.; Silva, M. M.; Silva, C. J.; Smith, M. J.; Assunção, M.; Alcácer, L. *J. Alloys Compd.* **1998**, *275-277*, 21. (b) Carlos, L. D.; de Zea Bermudez, V.; Duarte, M. C.; Silva, M. M.; Silva, C. J.; Smith, M. J.; Assunção, M.; Alcácer, L. *Physics and Chemistry of Luminescent Materials VI*; Ronda, C., Welker, T., Eds.; The Electrochemical Society Proceedings 97-29; San Francisco, 1997; p 352.

(21) (a) Ribeiro, S. J. L.; Dahmouche, K.; Ribeiro, C. A.; Santilli, C. V.; Pulcinelli, S. H. *J. Sol-Gel Sci. Technol.*, in press. (b) Franville, A. C.; Zambon, D.; Mahiou, R.; Chou, S.; Troin, Y.; Cousseins, J. C. *J. Alloys Compd.* **1998**, *275-277*, 831.

(22) (a) Armand, M.; Poinsignon, C.; Sanchez, J.-Y.; de Zea Bermudez, V.; Frenc Patent 91 11349, 1991. (b) De Zea Bermudez, V. Ph.D. Thesis, University of Grenoble, France, 1992. (c) De Zea Bermudez, V.; Baril, D.; Sanchez, J.-Y.; Armand, M.; Poinsignon, C. *Optical Materials Technology for Energy Efficiency and Solar Energy Conversion XI: Chromogenics for Smart Windows*; Hugot-Le Goff, A., Granqvist, C.-G., Lampert, C. M., Eds.; Proceedings SPIE 1728; SPIE: Bellingham, Washington, 1992; p 180.

(23) Canham, L. T. *Appl. Phys. Lett.* **1990**, *57*, 1046.

(24) (a) Chen, X.; Uttamchandani, D.; Trager-Cowan, C.; O'Donnell, K. P. *Semicond. Sci. Technol.* **1993**, *8*, 92. (b) Pifferi, A.; Taroni, P.; Torricelli, A.; Valentini, G.; Mutti, P.; Guisloti, G.; Zanghieri, L. *Appl. Phys. Lett.* **1997**, *70*, 348.

(25) Fauchet, P. M.; Peng, C.; Tsybeskov, L.; Vandyshev, J.; Dubois, A.; Raisanen, A.; Orlovski, T. E.; Brillson, L. J.; Fouquet, J. E.; Dexheimer, S. L.; Rehm, J. M.; McLendon, G. L.; Ettetdgui, E.; Gao, Y.; Seifert, F.; Kurinec, S. K. *Semiconductor Silicon/1994, 7th International Symposium on Silicon Materials Science and Technology*; Huff, H. R., Bergholtz, W., Sumino, K. Eds.; Electrochemical Society Proceedings 94-10; San Francisco, 1994; p 499.

(26) (a) Cameron, A.; Chen, X.; Trager-Cowan, C.; Uttamchandani, D.; O'Donnell, K. P. *Optical Properties of Low Dimensional Silicon Structures*; Bensahel, D. C., Canham, L. T., Ossicini, S., Eds.; Academic Press: Amsterdam, 1993. (b) Ventura, P. J.; Carmo, M. C.; O'Donnell, K. P. *J. Appl. Phys.* **1995**, *77*, 323.

(27) (a) Brandt, M. S.; Fuchs, H. D.; Stutzmann, M.; Weber, J.; Cardona, M. *Solid State Commun.* **1992**, *81*, 307. (b) Stutzmann, M.; Brandt, M. S.; Rosenbauer, M.; Weber, J.; Fuchs, H. D. *Phys. Rev. B* **1993**, *47*, 4806.

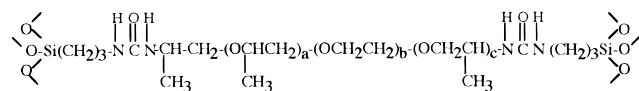
(28) Brus, L. J. *J. Phys. Chem.* **1994**, *98*, 3575.

(29) (a) Matsumoto, N. *Semiconductor Silicon/1994, 7th International Symposium on Silicon Materials Science and Technology*; Huff, H. R., Bergholtz, W., Sumino, K., Eds.; Electrochemical Society Proceedings 94-10; San Francisco, 1994; p 461. (b) Matsumoto, N.; Takeda, K.; Teramae, H.; Fujino, M. *International Topical Workshop on Advances in Silicon-Based Polymer Science*, Hawaii, 1987; Advances in Chemistry Series 224; American Chemical Society: Washington, DC, 1990. (c) Miller, R. D.; Michl, J. *J. Chem. Rev.* **1989**, *89*, 1359.

(30) Furukawa, K.; Fujino, M.; Matsumoto, N. *Macromolecules* **1990**, *22*, 1697.

(31) (a) Furukawa, K.; Fujino, M.; Matsumoto, N. *Appl. Phys. Lett.* **1992**, *60*, 2744. (b) Heath, J. R. *Science* **1992**, *258*, 1131.

the undoped materials whose structure is



with  $a + c = 2.5$  and  $b = 40.5, 15.5,$  or  $8.5$ . The room-temperature infrared spectra displayed by these compounds are discussed in detail in part 1. Part 2 deals with the corresponding photoluminescence spectra.<sup>32</sup>

The analysis of the mid-FTIR spectra of the ureasils has enabled us to assess the changes in the conformation of the oxyethylene chains undergone after their inclusion into the inorganic backbone.

Ever since the mid-1950s, a considerable number of infrared and Raman spectroscopic studies<sup>33–49</sup> has been devoted to the assignment of the conformations<sup>50</sup> of the polymer chains in POE and its lower molecular weight analogue poly(ethylene glycol), PEG, in the crystalline state,<sup>33,35,36,38–40,43,48</sup> in the molten state,<sup>33–36,38,41–43,45</sup> and in solution.<sup>35,45,46,49</sup> One of the most important contributions to the field of POE-based complexes is attributed to Tadokoro et al.<sup>40</sup> who carried out vibrational and detailed X-ray diffraction studies on the molecule of POE in the crystalline state. They concluded that this molecule has a helical structure. The polymer chain contains seven (OCH<sub>2</sub>CH<sub>2</sub>) units and two turns in the fiber identity period of 19.3 Å. According to the same authors, the conformations along the skeleton of the POE molecule are a succession of nearly *trans*-(CC–OC), *trans*-(CO–CC), and *gauche*-(OC–CO), also denoted (T<sub>2</sub>G), TTG, or 7<sub>2</sub> (seven chemical units and two turns of the helix in the fiber period). Matsuura et al.<sup>41</sup> have stated that although the *gauche* conformation of the O–(CH<sub>2</sub>)<sub>2</sub>–O moieties is retained in the molten state, some of the groups assume a *trans* conformation. Studies by infrared and NMR methods favor the TGT conformation for the COCCOC sequence of crystalline PEG in aqueous solutions.<sup>46</sup> The NMR spectra of PEG in the molten state and in solutions of chloroform and water were analyzed by Connor et al.<sup>51</sup> who found that the *gauche* form of the CH<sub>2</sub>CH<sub>2</sub> bond is more stable than

the *trans* form. Dipole moment studies of POEs in solutions of carbon tetrachloride and dioxane have been also carried out,<sup>52</sup> but their interpretation in terms of chain conformation is more equivocal.

When we initially recorded the mid-infrared spectra of the europium-doped ureasils with the goal of getting a better insight of the local structure around the dissolved lanthanide cation, we immediately recognized that the knowledge of the vibration modes arising from the urea moieties in the undoped materials was fundamental for the understanding of the spectral feature of the same materials after being doped with the Eu<sup>3+</sup> cation. It was clear that the absorption bands arising from the urea linkages were greatly affected by the inclusion of the europium salt. Given the scarcity of references in the literature dealing with the spectral signature of the urea group in polymers, we have decided to analyze this spectral region more deeply. A preliminary tentative assignment of the rather complex set of infrared absorption bands originating from the (–NHC(=O)NH–) moieties present in the ureasils is given in this paper.

The first calculation of the normal modes of vibration for the planar  $C_{2v}$  model of urea, NH<sub>2</sub>CONH<sub>2</sub>, and the assignment for the observed frequencies of crystalline urea and urea-*d*<sub>4</sub> is attributed to Yamaguchi et al.<sup>53</sup> Another normal coordinate analysis of NH<sub>2</sub>CONH<sub>2</sub> in the solid state and in acetonitrile solution was later proposed by Hadzi et al.<sup>54</sup> Nevertheless, since the ureasils may be chemically classified as diureas or asymmetric disubstituted ureas, our assignment will rely mostly on the exhaustive investigation carried out by Mido on the infrared spectra of 30 dialkylureas of the type RHNCONHR' in the solid state<sup>55</sup> and in chloroform solution<sup>56</sup> in the 4000–400 cm<sup>–1</sup> region. The position of the characteristic amide bands allowed Mido to postulate that the predominant molecular configuration of these compounds is the *trans*–*trans* form. The influence of the N-substituent was analyzed by Sudha et al.<sup>57</sup> who showed that *N,N*-arylalkylureas adopt the less energetic *trans*–*cis* form, in contrast to most *N,N*-disubstituted ureas. Mainly for comparison purposes, we have also based our assignment on the examination and interpretation of the infrared spectra of urea–formaldehyde resins and related model compounds suggested first by Myers<sup>58</sup> and later by Jada,<sup>59</sup> as well as on the very recent FTIR observations reported by Iijima et al.<sup>60</sup> of the orientation of dipolar urea bonds in polyurea during corona poling.

Two structural characteristics of the ureasils have induced us to consider also in our attribution, apart from Mido's studies,<sup>55,56</sup> the numerous in-depth spectroscopic studies of hydrogen bonding in polymer mixtures:<sup>61–67</sup>

(32) Carlos, L. D.; de Zea Bermudez, V.; Sá Ferreira, R. A.; Marques, L.; Assunção, M. *Chem. Mater.*, in press.

(33) Davidson, W. H. T. *J. Chem. Soc.* **1955**, 3270.

(34) Kuroda, Y.; Kubo, M. *J. Polym. Sci.* **1957**, 26, 323.

(35) Kuroda, Y.; Kubo, M. *J. Polym. Sci.* **1959**, 36, 453.

(36) White, H. F.; Lovell, C. M. *J. Polym. Sci.* **1959**, 41, 369.

(37) Miyake, A. *J. Am. Chem. Soc.* **1960**, 82, 3040.

(38) Yoshihara, T.; Tadokoro, H.; Murahashi, S. *J. Chem. Phys.* **1964**, 41 (9), 2902.

(39) Matsuura, H.; Miyazawa, T.; Machida, K. *Spectrochim. Acta* **1973**, 29A, 771.

(40) Tadokoro, H.; Chatani, Y.; Yoshihara, T.; Tahara, S.; Murahashi, S. *Makromol. Chem.* **1964**, 74, 109.

(41) Matsuura, H.; Miyazawa, T. *J. Polym. Sci.* **1969**, 7A (2), 1735.

(42) Machida, K.; Miyazawa, T. *Spectrochim. Acta* **1964**, 20, 1865.

(43) Matsuura, H.; Miyazawa, T. *Spectrochim. Acta* **1967**, 23A, 2433.

(44) Matsuura, H.; Miyazawa, T. *Bull. Chem. Soc. Jpn.* **1968**, 41, 1798.

(45) Koenig, J. L.; Angood, A. C. *J. Polym. Sci.* **1970**, 8A (2), 1787.

(46) Liu, K.-J.; Parsons, J. L. *Macromolecules* **1969**, 2 (5), 529.

(47) Miyazawa, T. *J. Polym. Sci.* **1961**, 55, 215.

(48) Miyazawa, T.; Fukushima, K.; Ideguchi, Y. *J. Chem. Phys.* **1964**, 37 (12), 2764.

(49) Takahashi, Y.; Tadokoro, A. *Macromolecules* **1973**, 6 (5), 672.

(50) Tadokoro, H. *Structure of Crystalline Polymers*, John Wiley & Sons: 1979.

(51) Connor, T. M.; McLauchlan, K. A. *J. Phys. Chem.* **1965**, 69 (6), 1888.

(52) Uchida, T.; Kurita, Y.; Koizumi, N.; Kubo, M. *J. Polym. Sci.* **1956**, 21, 313.

(53) Yamaguchi, A.; Miyazawa, T.; Shimanouchi, T.; Mizushima, S. *Spectrochim. Acta* **1957**, 10, 170.

(54) Hadzi, Z.; Kidric, J.; Knezevic, Z. V.; Barlic, B. *Spectrochim. Acta* **1976**, 32A, 693.

(55) Mido, Y. *Spectrochim. Acta* **1972**, 28A, 1503.

(56) Mido, Y. *Spectrochim. Acta* **1972**, 29A, 431.

(57) Sudha, L. V.; Sathyanarayana, D. N. *J. Mol. Struct.* **1984**, 125, 89.

(58) Myers, G. E. *J. Appl. Polym. Sci.* **1981**, 26, 747.

(59) Jada, S. S. *J. Appl. Polym. Sci.* **1988**, 35, 1573.

(60) Iijima, M.; Ukishima, S.; Iida, K.; Takahashi, Y.; Fukada, E. *Jpn. J. Appl. Phys.* **1995**, 34, L65.



(1) the hybrid nature of the ureasils, whose structure involves flexible polyether chains trapped between rigid blocks of silica by means of hard urea cross-links; (2) the well-known exceptionally strong self-association of urea compounds originating from the presence in the urea moiety of three active centers capable of participating in highly directional hydrogen bonds.

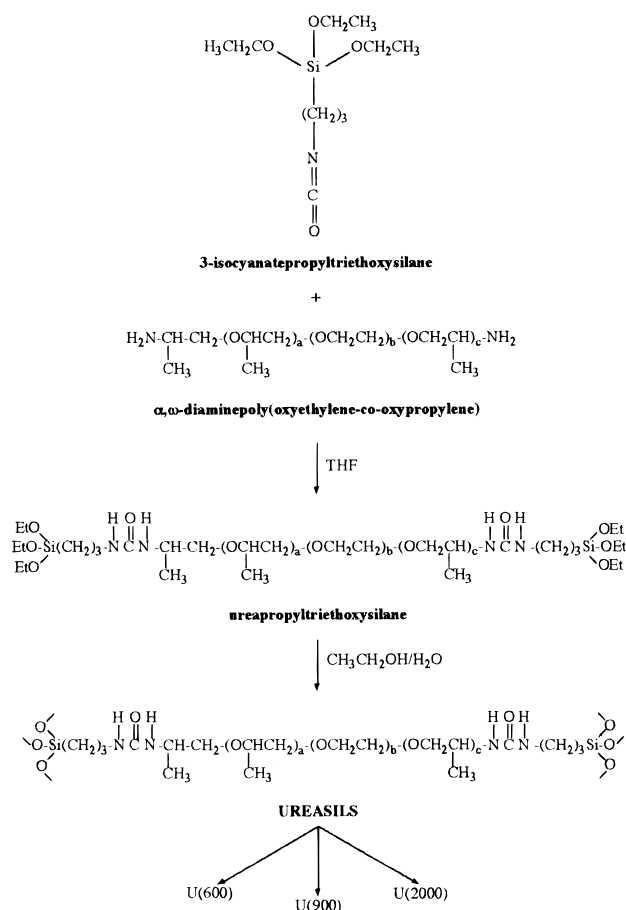
Intimate mixing of two polymers at the molecular level is attained if the interaction takes place between a strongly self-associated polymer (e.g., polyurethanes and polyamides) and a weakly self-associated one containing donor sites, such as oxygen or nitrogen atoms, capable of forming strong hydrogen bonds. Polyethers belong to the last category. We believe that there is a great resemblance between the ureasils and the extensively hydrogen-bonded polyurethane block polymers. The latter materials are known to be composed of alternating low glass transition soft segments (generally polyethers or polyesters) and more rigid, polar urethane ( $-\text{HNC}(=\text{O})\text{O}-$ ) hard segments formed from the extension of a diisocyanate (often aromatic) with low molecular weight diols. The donor sites are the N-H groups of the urethane linkages, and the hydrogen bond acceptors may be either the hard urethane segments (the carbonyl of the urethane groups) or the soft segments (ester carbonyls or ether oxygens).

Our analysis is mainly devoted to the study of the influence of the oxyethylene chain length on the frequency and intensity of the bands arising from the urea cross-links. The procedure adopted has been to closely inspect these bands in terms of the absorption bands characteristic of the amide structure ( $-\text{HNC}(=\text{O})-$ ), in particular the amide I, II, III, and V bands,<sup>68</sup> and to compare our experimental results with those widely referred for related materials.<sup>61-67</sup>

## Experimental Section

**Synthesis.** In the preliminary stage of the preparation of the ureasils a covalent bond between the alkoxysilane precursor (3-isocyanatepropyltriethoxysilane, ICPTES) and the oligopolyoxyethylene segment was formed by reacting the isocyanate group of the former compound with the terminal amine groups of doubly functional amines ( $\alpha,\omega$ -diaminepoly(oxyethylene-co-oxypropylene)) in tetrahydrofuran, THF (Scheme 1). A urea cross-linked organic-inorganic hybrid precursor—so-called ureapropyltriethoxysilane, UPTES—was thus obtained. The three diamines used in this study are commercially designated as Jeffamine ED-2001 (with  $a + c = 2.5$  and  $b = 40.5$ ), Jeffamine ED-900 (with  $a + c = 2.5$  and  $b = 15.5$ ), and Jeffamine ED-600 (with  $a + c = 2.5$  and  $b = 8.5$ ). In the second stage of the synthesis, a mixture of ethanol and

## Scheme 1. Synthesis of the Ureasils



water—the solvents that start the hydrolysis and condensation reactions that lead to the formation of the xerogels—was added to the UPTES solution (Scheme 1).

**Step 1. Synthesis of the Ureasil Precursor UPTES.** An amount of 2.5 g of Jeffamine ED-2001 (or Jeffamine ED-900 or Jeffamine ED-600) was dissolved with stirring in 10 mL of THF. A volume of 0.625 mL (or 1.388 or 2.081 mL, respectively) of ICPTES was added to this solution in a fume cupboard. The flask was sealed and the solution stirred overnight. The grafting process was infrared-monitored: as the reaction proceeds, the intensity of the very strong and sharp absorption band located at about  $2274\text{ cm}^{-1}$ , attributed to the vibration of the  $\equiv\text{Si}(\text{CH}_2)_3\text{NCO}$  group, progressively decreases, while that of bands produced by urea groups increases.

**Step 2. Synthesis of the Ureasils.** A mixture of 0.582 mL (or 1.293 or 1.941 mL, respectively) of ethanol and 0.067 mL (or 0.149 or 0.225 mL, respectively) of water (molar proportion 1 ICPEs: 4  $\text{CH}_3\text{CH}_2\text{OH}$ : 1.5  $\text{H}_2\text{O}$ ) was added to the solution prepared in step 1. The mixture was stirred in a sealed flask for 30 min and then cast into a Teflon mold and left in a fume cupboard for 24 h. The mold was covered with Parafilm perforated with a syringe needle in order to ensure the slow evaporation of the solvents. After a few hours, gelation occurred and the mold was transferred to an oven at  $40\text{ }^\circ\text{C}$  for a period of 7 days. The sample was then aged at about  $80\text{ }^\circ\text{C}$  for 3 weeks to form a transparent, fairly rigid and brittle elastomeric monolithic film with a yellowish coloration. The final materials, i.e., the ureasils, have been identified by the designation U(Y), where U originates from the word "urea" and Y = 2000, 900, or 600, indirectly indicating the length of the oligopolyoxyethylene chains.

**Materials and Methods.** Jeffamine ED-2001 (Fluka) was dried under vacuum for several days prior to being analyzed. Jeffamine ED-600 (Fluka),  $\text{CH}_3\text{CH}_2\text{OH}$  (Merck), and THF (Merck) were kept in contact with dried molecular sieves prior to being used. Jeffamine ED-900 (Fluka) and ICPTES (Fluka)

(61) (a) Skrovanek, D. J.; Howe, S. E.; Painter, P. C.; Coleman, M. M. *Macromolecules* **1985**, *18*, 1676. (b) Skrovanek, D. J.; Painter, P. C.; Coleman, M. M. *Macromolecules* **1986**, *19*, 699.

(62) Coleman, M. M.; Lee, K. H.; Skrovanek, D. J.; Painter, P. C. *Macromolecules* **1986**, *19*, 2149.

(63) Lee, H. S.; Wang, Y. K.; Hsu, S. L. *Macromolecules* **1987**, *20*, 2089.

(64) Lee, H. S.; Wang, Y. K.; Macknight, W. J.; Hsu, S. L. *Macromolecules* **1988**, *21*, 270.

(65) Coleman, M. M.; Skrovanek, D. J.; Hu, J.; Painter, P. C. *Macromolecules* **1988**, *21*, 59.

(66) Zharkov, V. V.; Strikovskiy, A. G.; Verteletskaya, T. E. *Polymer* **1993**, *34* (5), 938.

(67) (a) Bradley, R. H.; Mathieson, I.; Byrne, K. M. *J. Mater. Chem.* **1997**, *7* (12), 2477. (b) Church, J. S.; Corino, G. L.; Woodhead, A. L. *J. Mol. Struct.* **1998**, *440*, 15.

(68) Miyazawa, T.; Shimanouchi, T.; Mizushima, S.-I. *J. Chem. Phys.* **1956**, *24* (2), 408.

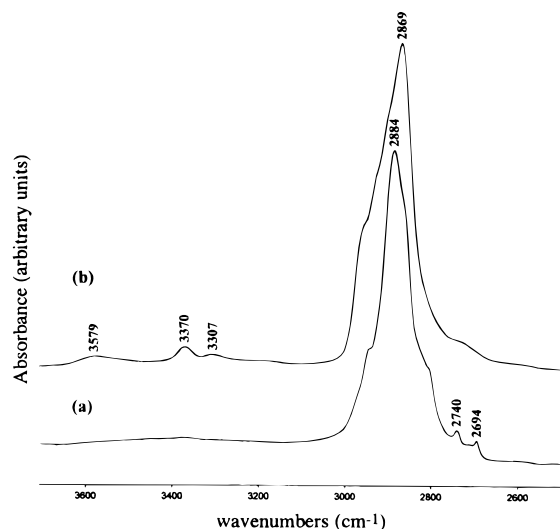


**Figure 1.** Room-temperature high-frequency mid-infrared spectra of Jeffamine ED-2001 (a) and Jeffamine ED-600 (b).

were used as received. Distilled water was used in all experiments.

Mid-infrared spectra were acquired at room temperature using a Unicam FT-IR system. The spectra were collected over the range 4000–400  $\text{cm}^{-1}$  by averaging 60 scans at a maximum resolution of 4  $\text{cm}^{-1}$ . Solid samples (2 mg) were finely ground and analyzed by dispersing them in approximately 175 mg of dried spectroscopic grade potassium bromide (KBr, Merck) by the pressed-disk technique. The disks were vacuum-dried at 90 °C for a long period of time in order to reduce the levels of solvent and adsorbed water in the samples prior to recording the spectra under ambient conditions. Consecutive spectra were recorded until reproducible results were obtained. The evaporation was infrared-monitored in the OH region. Liquid samples were spread between two NaCl windows that were immediately sealed with Teflon tape to exclude atmospheric moisture. To evaluate complex band envelopes and to identify underlying component bands of the mid-infrared spectra, the curve-fitting procedure in the ORIGIN computer software for IBM PC compatible computers has been used. Band shapes have been described by Gaussian-type functions. Unambiguous results are difficult to obtain, since they depend strongly on the starting parameters. Unless stated otherwise, the curve-fitting procedure has been used mostly to confirm bands already observed as shoulders.

## Results and Discussion

The room-temperature high- and low-frequency mid-infrared spectra of Jeffamine ED-2001 are shown in Figures 1a and 2a, respectively. The wavenumbers of the mid-infrared absorption bands obtained for this diamine and those reported in the literature for tetra(ethyleneglycol) dimethyl ether (TEGDME,  $\text{CH}_3\text{O}(\text{CH}_2\text{CH}_2\text{O})_4\text{CH}_3$ ), hepta(ethyleneglycol) dimethyl ether (HEGDME,  $\text{CH}_3\text{O}(\text{CH}_2\text{CH}_2\text{O})_7\text{CH}_3$ ), and poly(ethylene glycol) (PEG,  $\text{HO}(\text{CH}_2\text{CH}_2\text{O})_n\text{H}$ ) in the crystalline state are listed in Table 1. The assignments of the vibrational bands of the tetramer, heptamer, and high molecular weight PEG quoted in Table 1 are based on the attribution proposed by Matsuura et al.<sup>39</sup> The room-temperature high- and low-frequency mid-infrared spectra of Jeffamine ED-600 are represented in Figures 1b and 2b, respectively. In Table 2, the frequencies of the mid-infrared absorption bands of TEGDME, HEGDME, and PEG in the liquid state reported by several authors<sup>41,42</sup>

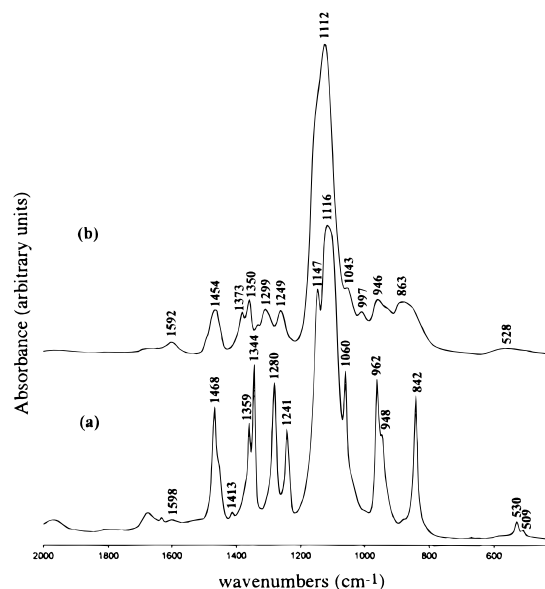


**Figure 2.** Room-temperature low-frequency mid-infrared spectra of Jeffamine ED-2001 (a) and Jeffamine ED-600 (b).

are compared with those obtained for Jeffamine ED-600. The room-temperature high- and low-frequency mid-infrared spectra of the ureasils are shown in Figures 3 and 4, respectively. Parts a–c of Figure 5 report the curve-fitting results of the room-temperature amide I region of U(600), U(900), and U(2000), respectively. The attributions proposed for the bands observed in the mid-infrared spectra of the ureasils are given in Table 3.

**1. Spectral Consequences Resulting from the Incorporation of the Oxyethylene Chains of Jeffamine ED-2001 into the Silica Backbone.** If the bands at 3370 and 1598  $\text{cm}^{-1}$ , whose attribution will be discussed below, are excluded from the spectrum of Jeffamine ED-2001 (Figures 1a and 2a and Table 1), the resulting spectral feature is essentially that of crystalline high molecular weight PEG (Table 1). There are also remarkable similarities between the spectrum of this diamine and those of TEGDME and HEGDME in the crystalline state (Table 1). This is not surprising considering that the average number of oxy(ethylene) units in this diamine is approximately 40. The coincidence of the wavenumber of many bands is not casual, since the tetramer and heptamer contain four and seven ( $\text{OCH}_2\text{CH}_2$ ) units, which correspond, respectively, to  $1/10$  and about  $1/5$  of the number of repeat units of Jeffamine ED-2001.

The spectrum of Jeffamine ED-2001 is deeply modified after incorporating this diamine into the silica network, as it may be immediately inferred from Figures 3c and 4c. In the hybrid material, most of the bands are broad and many have become ill-defined. Furthermore, although some of the bands of Jeffamine ED-2001 undergo minor shifts, others simply disappear.

At high frequencies the spectra of the ureasils (Figure 3 and Table 3) closely resemble not only those of PEG, TEGDME, and HEGDME in the liquid state (Table 2) but also that of Jeffamine ED-600 (Figure 1b and Table 2), which is a viscous liquid at room temperature.

The inspection of the spectral region between 1500 and 800  $\text{cm}^{-1}$  reveals that the most striking effect upon melting of PEG is the presence of four new weak

**Table 1. Room Temperature Mid-Infrared Spectra of Tetra(ethyleneglycol) Dimethyl Ether (TEGDME, CH<sub>3</sub>O(CH<sub>2</sub>CH<sub>2</sub>O)<sub>4</sub>CH<sub>3</sub>), Hepta(ethyleneglycol) Dimethyl Ether (HEGDME, CH<sub>3</sub>O(CH<sub>2</sub>CH<sub>2</sub>O)<sub>7</sub>CH<sub>3</sub>), and Poly(ethylene glycol) (PEG, HO(CH<sub>2</sub>CH<sub>2</sub>O)<sub>n</sub>H) in the Crystalline State and of Jeffamine ED-2001<sup>a</sup>**

crystalline TEGDME <sup>39</sup>	crystalline HEGDME <sup>39</sup>	crystalline PEG <sup>39</sup>	Jeffamine ED-2001	attribution	
			3370 w	$\nu_a$ NH <sub>2</sub>	
2973 S	2973 m			$\nu_a$ CH <sub>3</sub>	
2958 m	2953 m	2950 m	2951 sh	$\nu_a$ CH <sub>2</sub>	
1923 S	2922 sh		2924 sh	$\nu_s$ CH <sub>3</sub>	
2893 vS	2890 vS	2890 vS		$\nu_s$ CH <sub>2</sub>	
		2885 vS	2884 vS		
2876 sh			2859 sh		
2864 sh	2863 sh	2865 S			
2851 sh					
2825 S	2819 m	2825 sh			
2810 sh		2805 sh	2814 sh	combination vibrations	
2790 w					
2769 w					
2743 w	2743 w	2740 w	2740 w		
2727 w					
2708 w		2710 w			
2701 w	2698 w	2695 w	2694 w		
			1963 wb		
			1675 w		
			1598 wb		$\delta$ NH <sub>2</sub>
1477 sh				CH <sub>2</sub> scissoring and CH <sub>3</sub> deformation	
1468 m	1468 m	1470 m	1468 m		
1458 w		1463 m			
			1457 m		
1449 w	1447 w	1453 w	1452 sh		
1441 w				CH <sub>2</sub> wagging	
1431 w					
	1420 w				
1414 w	1412 w	1415 w	1413 w		
1383 w	1385 w				
1370 w	1366 w				
1358 w	1361 m	1364 m	1359 m		
1352 w	1350 w	1345 S	1344 S		
1282 S	1280 S	1283 m	1280 m		
1241 w		1244 m	1241 m		CH <sub>2</sub> twisting
1235 w	1235 w	1236 w		CH <sub>3</sub> rocking	
1200 m	1198 w				
1160 w	1160 sh				
1147 S	1147 S	1149 S	1147 S		$\nu$ CO + rCH <sub>2</sub>
1127 m					$\nu$ CO
1111 S	1111 S	1119 S	1116 vS		
1100 S		1102 S			$\nu$ CO, $\nu$ CC, rCH <sub>2</sub>
1085 sh					
1073 sh					
1067 w	1062 m	1062 m	1060 m		
1028 m	1030 m			$\nu$ O-CH <sub>3</sub>	
967 w	961 sh	963 S	962 S	$\nu$ CC, rCH <sub>2</sub>	
	954 sh				
948 w		947 m	948 m	$\nu$ CO, rCH <sub>2</sub>	
939 w	938 m				
859 sh					
853 S	853 m				
845 m					
836 sh	842 m	844 S	842 S		
816 sh					
586 w	586 w				
562 m					
	557 w				COC and CCO bending
	538 w				
532 w	528 w	529 w	530 vw		
521 w					
	512 w	508 w	509 vw		

<sup>a</sup> Frequencies in cm<sup>-1</sup>; vS, very strong; S, strong; m, medium; w, weak; vw, very weak; sh, shoulder.

absorption bands in the infrared spectrum (Table 2). According to Matsuura et al.,<sup>41</sup> these bands are characteristic of the molten or amorphous state and are due to disordered regions. The first band is the one situated at 1326 cm<sup>-1</sup> (Table 2). It is downshifted to 1322 cm<sup>-1</sup> in the spectra of Jeffamine ED-600 and U(600) and does not show up in the spectra of U(900) and U(2000). The

**Table 2. Room-Temperature Mid-Infrared Spectra of Tetra(ethyleneglycol) Dimethyl Ether (TEGDME, CH<sub>3</sub>O(CH<sub>2</sub>CH<sub>2</sub>O)<sub>4</sub>CH<sub>3</sub>), Hepta(ethyleneglycol) Dimethyl Ether (HEGDME, CH<sub>3</sub>O(CH<sub>2</sub>CH<sub>2</sub>O)<sub>7</sub>CH<sub>3</sub>), and Poly(ethylene glycol) (PEG, HO(CH<sub>2</sub>CH<sub>2</sub>O)<sub>n</sub>H) in the Liquid State and of Jeffamine ED-600<sup>a</sup>**

liquid TEGDME <sup>42</sup>	liquid HEGDME <sup>42</sup>	liquid PEG <sup>41</sup>	Jeffamine ED-600	attribution	
			3579 vwb		
			3370 vw	$\nu_a$ NH <sub>2</sub>	
			3307 vw	$\nu_s$ NH <sub>2</sub>	
2975 sh			2963 sh	$\nu_a$ CH <sub>3</sub>	
2920 sh		2930 sh	2936 sh	$\nu_a$ CH <sub>2</sub>	
			2906 sh		
2880 S	2880 S	2865 S	2869 S	$\nu_s$ CH <sub>2</sub>	
2820 sh				combination vibrations	
		2730 sh			
			1592 vw	$\delta$ NH <sub>2</sub>	
		1485 sh	1482 sh	CH <sub>2</sub> scissoring and CH <sub>3</sub> deformation	
			1470 sh		
1456 m	1457 m	1460 m	1454 m		
			1373 m	CH <sub>2</sub> wagging	
1353 m	1354 m	1352 m	1350 m		
1328 w	1328 w	1326 w	1322 w	liquid state	
1299 m	1300 m	1296 m	1299 m	CH <sub>2</sub> twisting	
1248 m	1252 m	1249 m	1249 m		
1199 m	1200 w				
1140 sh	1140 sh	1140 sh	1144 sh		$\nu$ CO + rCH <sub>2</sub>
1109 S	1110 S	1107 S	1112 vS		$\nu$ CO
1042 sh	1035 w	1038 m	1043 m	$\nu$ CO, $\nu$ CC, rCH <sub>2</sub>	
1028 w				liquid state	
985 w	986 w	992 w	997 w		
965 sh					
943 w	948 w	945 m	946 m		$\nu$ CC, rCH <sub>2</sub>
		915 sh		liquid state	
850 m	852 m	855 m	863 vwb	$\nu$ CO, rCH <sub>2</sub>	
		810 sh		liquid state	
540 m	525 m		528 vwb	COC+CCO bending	

<sup>a</sup> Frequencies in cm<sup>-1</sup>; vS, very strong; S, strong; m, medium; w, weak; vw, very weak; sh, shoulder; b, broad.

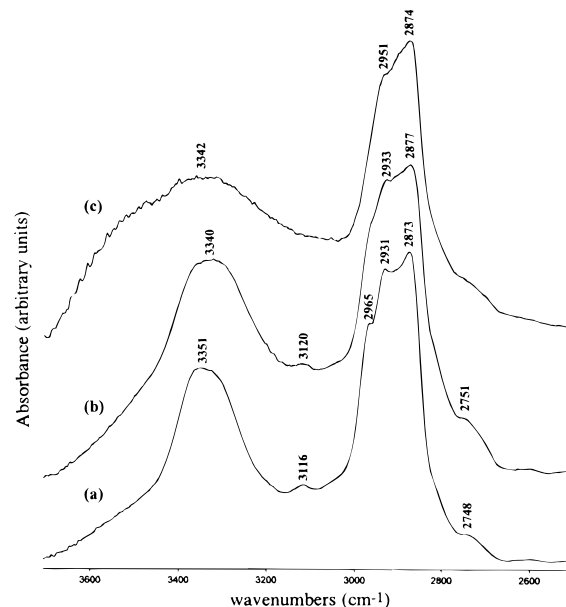


**Figure 3.** Room-temperature high-frequency spectra of the undoped ureasils: (a) U(600), (b) U(900), and (c) U(2000).

second band, at 992 cm<sup>-1</sup> (Table 2), is also observed in the liquid oligomers, at lower wavenumber, and in Jeffamine ED-600, though slightly upshifted (997 cm<sup>-1</sup>). It is not detected in the spectra of the ureasils. The shoulder produced by U(600) and U(900) at 921 and 922 cm<sup>-1</sup>, respectively, will be connected with the third band

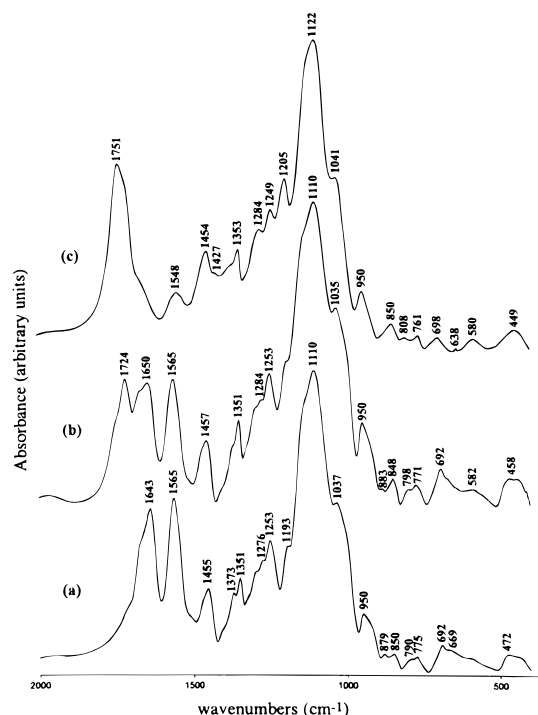


**Figure 4.** Room-temperature low-frequency spectra of the undoped ureasils: (a) U(600), (b) U(900), and (c) U(2000).

of PEG indicative of the amorphous state at  $915\text{ cm}^{-1}$  (Table 2). The fourth band of liquid PEG associated with the molten state, a shoulder at  $810\text{ cm}^{-1}$  (Table 2), is not detected in any of the spectra of the compounds under analysis.

Unlike the situation found in the spectrum of Jeffamine ED-2001 for which the  $(\text{OCH}_2\text{CH}_2)$ -based chains are expected to take regularly ordered conformations, the effects just described and discussed regarding the spectrum of U(2000) provide conclusive evidence that the oligopoly(oxyethylene) chains of this organic-inorganic hybrid material have changed from a helical structure to a new, less ordered, though not completely disordered, structure. In fact, the spectrum of U(2000) is substantially identical not only to the spectrum of liquid PEG but also to the spectra of Jeffamine ED-600 or U(600), which contain fewer repeat units (about 8.5) than the ones introduced in U(2000) (about 40.5). The bands indicative of the liquid state, i.e.,  $1326$ ,  $992$ ,  $915$ , and  $810\text{ cm}^{-1}$ , are nevertheless missing in the spectrum of U(2000). Although the considerable broadening and consequent reduction of the apparent intensity of most of the bands produced by the oxyethylene moieties indicate the partial relaxation of the crystal structure of Jeffamine ED-2001 upon synthesis of the hybrid compound, the absence of the liquid bands referred above suggests that although the molecules as units are more or less free to rotate about their skeletal axis, they are semirigid about the individual skeletal bonds. This is logical considering that the grafting procedure markedly reduces their mobility. The semirigid molecules probably tend to form ordered regions in the ureasil to give the material some short-range order. Consequently, the changes in the structure of the backbone of the polyether chains of Jeffamine ED-2001 upon inclusion in the silica network are not as complete as those

**Table 3.** Room-Temperature Mid-Infrared Spectra of the Undoped Ureasils U(600), U(900), and U(2000)<sup>a</sup>

U(600)	U(900)	U(2000)	attribution
3351 m	3340 m	3342 mb	$\nu\text{NH}$ hydrogen-bonded amide II $\times 2$
3116 w	3120 w		
2965 sh			$\nu_a\text{CH}_3$
2931 S	2933 S	2951 sh	$\nu_a\text{CH}_2$
2873 S	2877 S	2874 S	$\nu_s\text{CH}_2$
2748 sh	2751 sh	2733 sh	combination vibrations
	1963 wb		
	1751 sh	1750 S	amide I
1715 sh	1721 S	1716 sh	
1671 sh	1674 S	1677 sh	
1642 S	1641 sh		amide II
1565 S	1565 S	1548 w	
1476 sh			$\text{CH}_2$ scissoring and $\text{CH}_3$ deformation
1455 m	1457 m	1454 m	
		1427 m	
1373 m	1373 sh	1380 sh	$\text{CH}_2$ wagging
1351 m	1351 m	1353 m	
1322 w			liquid state
1301 m	1303 sh		
1276 m	1284 m	1284 m	amide III
1253 m	1253 m	1249 m	$\text{CH}_2$ twisting
1193 m	1197 m	1205 S	
1151 sh	1145 sh	1148 sh	$\nu\text{CO} + \text{rCH}_2$
1110 vS	1110 vS	1122 vS	$\nu\text{CO}$
1037 m	1035 S	1041 S	$\nu\text{CO}$ , $\nu\text{CC}$ , $\text{rCH}_2$
950 w	950 m	950 w	$\nu\text{CC}$ , $\text{rCH}_2$
921 sh	922 sh		liquid state
879 vw	883 vw	879 sh	$\nu\text{CO}$ , $\text{rCH}_2$
850 m	848 vw	850 w	
790 vw	798 vw	808 vw	
775 vw	771 vw	761 vw	amide VI
692 vw	692 w	698 vw	amide V
669 vwb			
		638 vw	$\delta(\text{N-C-N})$
	582 wb	580 vw	
		528 vwb	$\text{COC} + \text{CCO}$ bending
472 vwb	484 vw		
	458 wb	449 wb	

<sup>a</sup> Frequencies in  $\text{cm}^{-1}$ ; vS, very strong; S, strong; m, medium; w, weak; vw, very weak; sh, shoulder; b, broad.

undergone by PEG upon melting. In other words, the polymer chains in U(2000) have more segmental mobility than in the diamine, but the individual molecules have not achieved total mobility. Furthermore, the absence of the liquid bands in the spectrum of the ureasil, particularly the band at  $992\text{ cm}^{-1}$ , eliminates the possibility of the trans structure characteristic of the molten state; i.e., the conformation of the oligopolyether chains of Jeffamine ED-2001 after being incorporated into the silica matrix retains to a large degree the TGT sequence characteristic of the crystalline state of the diamine. Another piece of spectroscopic evidence supports our claim. The most intense band of the spectrum of U(2000), attributed to the C–O stretching vibration, is found at  $1122\text{ cm}^{-1}$ , closer to the position observed in the spectrum of crystalline PEG ( $1119\text{ cm}^{-1}$ ) than in that of liquid PEG ( $1107\text{ cm}^{-1}$ ). The X-ray powder diffraction pattern of U(2000)<sup>20,32</sup> corroborates these spectroscopic results.

Let us now analyze the lower weight analogues of U(2000). Our spectroscopic data clearly prove that in both Jeffamine ED-600 and U(600) the oxyethylene chains do attain complete disorder. A situation similar to that encountered in liquid PEG is present, as indicated by the presence of bands attributed to the molten state (at  $1322\text{ cm}^{-1}$  in both compounds and also at  $921\text{ cm}^{-1}$  in U(600)), thus implying the contribution



of the trans conformations. The amorphous, disorganized nature of U(600) is illustrated in its diffractogram.<sup>32</sup> Finally, we may state that the general physicochemical behavior of U(900) is very similar to that of U(600). Although only one band indicative of the liquid state is detected in its infrared spectrum (at 922 cm<sup>-1</sup>), the compound gives rise to a spectral signature that basically resembles that displayed by liquid PEG or by U(600). This result is supported by X-ray powder diffraction.<sup>32</sup>

**2. Spectral Analysis of Bands Produced by Particular Groups in Jeffamine ED-2001, in Jeffamine ED-600, and in the Ureasils.** *Bands Originating from Amine Groups.* Owing to the high number of (OCH<sub>2</sub>CH<sub>2</sub>) repeat units in the structure of Jeffamine ED-2001, the terminal NH<sub>2</sub> groups of this diamine give rise to only two absorption bands (Figure 1a and Table 1): a very weak ill-defined one at 3370 cm<sup>-1</sup> and a weak broad one at 1598 cm<sup>-1</sup>, which are assigned to the asymmetric stretching vibration and deformation of the NH<sub>2</sub> groups, respectively.<sup>69-71</sup> The symmetric component of the NH stretching vibration is not detected. The other most characteristic absorption bands of aliphatic primary amines with secondary  $\alpha$ -carbons are also missing in the spectrum of Jeffamine ED-2001:<sup>71</sup> (1) the strong band produced by the asymmetric stretching vibration of the C-N group, expected at 1040  $\pm$  3 cm<sup>-1</sup>, overlaps the very strong band at 1116 cm<sup>-1</sup>; (2) the pair of broad and strong bands originating from the asymmetric and symmetric NH<sub>2</sub> bending modes found at 794  $\pm$  16 and 840  $\pm$  11 cm<sup>-1</sup>, respectively, is masked by the strong band at 842 cm<sup>-1</sup>.

In the high-frequency spectral region Jeffamine ED-600 displays two weak bands at 3370 and 3307 cm<sup>-1</sup> that are attributed to the asymmetric and symmetric stretching vibrations of the terminal NH<sub>2</sub> groups of the diamine<sup>69-71</sup> (Figure 1b and Table 2). The well-known relationship proposed by Stewart<sup>71</sup>, i.e.,  $\bar{\nu}_{\text{sym}} = 0.98\bar{\nu}_{\text{asym}}$  holds here. Jeffamine ED-600 also gives rise to a weak absorption band at 1594 cm<sup>-1</sup>, assigned to the NH<sub>2</sub> deformation vibration.<sup>69-71</sup> Similar to what happened in the case of Jeffamine ED-2001, the strong infrared band assigned to the asymmetric stretching vibration of the C-N group expected at 1040  $\pm$  3 cm<sup>-1</sup><sup>71</sup> is again masked by the very strong band produced by the C-O stretching vibration situated in the spectrum of Jeffamine ED-600 at 1112 cm<sup>-1</sup>. In the 850-750 cm<sup>-1</sup> spectral region of the latter compound, a very weak single band is observed at 863 cm<sup>-1</sup>. It might originate either from the coupled vibration of the C-O stretching and CH<sub>2</sub> rocking modes or from the symmetric bending vibration of the NH<sub>2</sub> groups. However, considering the minor percentage of amine moieties in the compound, we have preferred to assign it to the former vibration modes, as mentioned previously.

*Bands Involving Silicon Atoms.* There is a minor percentage of silicon atoms in the ureasils (e.g., the silica precursor prepared from Jeffamine ED-2001 contains

92 carbon atoms between the urea bridges versus only 2 silicon atoms). The absorption bands resulting from the vibration of silicon-based bonds are thus expected to be less intense than those arising from the vibrations of the organic chains included in the hybrid materials.

To avoid water quenching, an extremely low molar ratio of water versus silica precursor was chosen in the sol-gel step of the synthesis procedure of the ureasils (i.e., 1.5 H<sub>2</sub>O:1ICPTES). It is thus highly probable that some unreacted ethoxysilane groups, Si-OCH<sub>2</sub>CH<sub>3</sub>, of the precursor remain in the materials because of incomplete hydrolysis. Taking into account the reversibility of the hydrolysis and condensation reactions of the sol-gel process, two situations are equally possible: (1) the original ethoxy groups of ICPTES could have remained or have been hydrolyzed to ethanol; (2) the original ethanol groups could have remained or been exchanged with silanol groups to form ethoxy ones. The ethoxy group gives rise to a strong doublet at 1100-1075 cm<sup>-1</sup> and two medium-intensity bands at 1175-1160 and 970-940 cm<sup>-1</sup>.<sup>70,72</sup> In the spectra of U(600), U(900), and U(2000) the doublet and the band between 1175 and 1160 cm<sup>-1</sup> are obscured by the very intense C-O stretching absorption and the strong coupled vibrations of the C-C stretching, C-O stretching, and CH<sub>2</sub> rocking modes that fall in the same range of frequencies (Figure 4 and Table 3). As to the lower frequency band, it is masked by the medium-to-weak intensity band at 950 cm<sup>-1</sup>, attributed to the stretching and rocking vibrations of the C-C and CH<sub>2</sub> groups, respectively.

The presence of residual silanol groups, Si-OH, a common situation in many sol-gel derived materials, reflects incomplete polycondensation. In the high-frequency region, free Si-OH groups usually give rise to a weak band at 3690 cm<sup>-1</sup>, which downshifts to 3400-3200 cm<sup>-1</sup> with hydrogen bonding producing a medium-intensity band.<sup>70,72</sup> The tetramethoxyortosilane, TMOS, derived xerogels prepared by Orcel et al.<sup>73</sup> absorb at 3750, 3660, and 3540 cm<sup>-1</sup> because of the stretching vibration of, respectively, free surface, internal, and hydrogen-bonded Si-OH groups. According to Ou et al.,<sup>74</sup> the shoulder found in the spectrum of the phenyl-modified silicate at 3606 cm<sup>-1</sup> should be attributed to hydrogen-bonded surface silanols. The silanol stretching bands in the spectra of the ureasils are not easily detected (Figure 3), since the complex broad feature observed at this range of frequencies may originate not only from the stretching vibration of Si-OH groups but also from the stretching vibration of the NH groups of the urea cross-links and from the stretching vibration of adsorbed water. In the case of U(2000) the ill-defined contour observed makes the identification especially difficult (Figure 3c). Silanols also absorb strongly at 950-830 cm<sup>-1</sup> because of the Si-OH stretching vibration.<sup>70,72</sup> In the spectra of the vinyl samples obtained by Ou et al.<sup>74</sup> this vibration mode gives rise to a strong band at 964 cm<sup>-1</sup> and in those of the phenyl-derived materials to a medium intensity one at 957 cm<sup>-1</sup>. In TMOS this band is seen at 950 cm<sup>-1</sup>.<sup>73</sup> In the spectra of the ureasils this band is masked by the broad

(69) Batista de Carvalho, L. A. E.; Amorim da Costa, A. M.; Duarte, M. L.; Teixeira-Dias, J. J. C. *Spectrochim. Acta* **1988**, *44A* (7), 723.

(70) (a) Nakanishi, K. *Infrared Absorption Spectroscopy: Practical*; Holden-Day, Inc.: San Francisco, 1962. (b) Colthup, N. B.; Daly, L. H.; Wiberley, S. E. *Introduction to Infrared and Raman Spectroscopy*, 3rd ed.; Academic Press: London, 1990.

(71) Stewart, J. E. *J. Chem. Phys.* **1959**, *30* (5), 1259.

(72) Smith, A. L. *Spectrochim. Acta* **1960**, *16*, 87.

(73) Orcel, G.; Phalippou, J.; Hench, L. L. *J. Non-Cryst. Solids* **1986**, *88*, 114.

(74) Ou, D. L.; Seddon, A. B. *J. Non-Cryst. Solids* **1997**, *210*, 187.



band at  $950\text{ cm}^{-1}$  assigned to the coupled vibration of the C–C stretching and  $\text{CH}_2$  rocking modes.

In short, infrared spectroscopy is not conclusive for the existence or absence of Si– $\text{OCH}_2\text{CH}_3$  or Si–OH groups in the ureasils. The latter should be much more easily distinguishable in the near-infrared overtone and combination region.

*Bands Originating from Urea Groups. NH Stretching Region.* The broadness of the hydrogen-bonded N–H band reflects a distribution of hydrogen-bonded N–H groups of varying strength dictated by distance and geometry. However, owing to the bad resolution and complexity of the spectra in the high-frequency region, absorption bands due to N–H group vibrations cannot be used for quantitative assessment of the hydrogen-bonded urea groups. Although this spectral region will not be discussed in detail in this work, several bands will be tentatively assigned. This attribution will be based mainly on the extensive infrared spectroscopic studies carried out on polyamides<sup>61</sup> and polyurethanes.<sup>62–66</sup> The word “free” in quotations will also be used here to describe urea N–H or C=O groups that are not directly hydrogen-bonded.

Amorphous polyamides are known to exhibit a weak shoulder at  $3444\text{ cm}^{-1}$  and a very broad band at  $3310\text{ cm}^{-1}$  that have been assigned to “free” and hydrogen-bonded N–H stretching modes, respectively.<sup>61</sup> Remarkably similar frequencies ( $3440$  and  $3320\text{ cm}^{-1}$ ) have been reported for simple linear semicrystalline aliphatic polyurethanes in this spectral region.<sup>62</sup> In the model polyurethanes investigated by Lee et al.<sup>63</sup> the same modes give rise to bands at slightly different frequencies ( $3450\text{ cm}^{-1}$  and from  $3330$  to as low as  $3200\text{ cm}^{-1}$ ). In polyurethane–ether blends the “free” N–H groups produce a band at  $3440\text{ cm}^{-1}$ , whereas the hydrogen-bonded one is found at approximately  $3340\text{ cm}^{-1}$ .<sup>65</sup> Jada has reported the presence of a very strong band at  $3346\text{ cm}^{-1}$  in the spectrum of 1,3-dimethylurea,  $(\text{CH}_3)_2\text{NHC}(=\text{O})\text{NH}(\text{CH}_3)$ .<sup>59</sup> In polyurea a single band is seen at  $3330\text{ cm}^{-1}$ .<sup>60</sup>

Although dialkylureas of the type  $\text{R}'\text{HNC}(=\text{O})\text{NHR}'$  are expected to produce only one band in the N–H stretching region,  $\text{RHNC}(=\text{O})\text{NHR}'$  diureas give rise to two distinct bands in this range of frequencies. In the spectra of the dialkylureas investigated by Mido these bands appear between  $3320$  and  $3380\text{ cm}^{-1}$  and are as a rule separated by approximately  $20$ – $60\text{ cm}^{-1}$ .<sup>55</sup> For instance, 1-methyl-3-*tert*-butylurea displays two bands at  $3376$  and  $3318\text{ cm}^{-1}$ .<sup>55</sup> According to the same author, this experimental evidence is attributable to the existence in the latter type of compounds of substituents of different sizes whose steric effect on the molecular structure creates an imbalance between both hydrogen bondings through the *trans*-amide hydrogens.

Since the ureasils belong to the second group of disubstituted ureas, two bands originating from the N–H stretching vibration should in principle be found in the high-frequency region of their spectra. A medium-intensity single broad band and a weak one are observed, respectively, at about  $3351$  and  $3116\text{ cm}^{-1}$  in the spectrum of U(600) (Figure 3a) and at  $3340$  and  $3120\text{ cm}^{-1}$  in the spectrum of U(900) (Figure 3b). The stronger band is undoubtedly associated with the stretching vibration of the secondary hydrogen-bonded N–H

groups of the urea bridges. Given its bad resolution, it is impossible to resolve it into two components. Mido encountered the same problem in the spectra of some dialkylureas.<sup>55</sup> We will assign the weaker band to an overtone of the  $1565\text{ cm}^{-1}$  band.<sup>69,70</sup> As for U(2000), it displays only a broad, ill-defined band centered at about  $3342\text{ cm}^{-1}$  in this spectral region (Figure 3c). Obviously, it is extremely difficult to distinguish the N–H groups from hydrogen bonds in the spectra of the ureasils.

*Bands in the Amide I Region.* The amide I mode is a highly complex vibration that involves the contribution of the C=O stretching, the C–N stretching, and the C–C–N deformation vibrations.<sup>68</sup> Unlike the N–H stretching vibration, the C=O stretching vibration is sensitive to the specificity and magnitude of hydrogen bonding. Thus, the amide I vibration consists of several components reflecting C=O groups in different environments.

Jada has attributed the band at  $1635\text{ cm}^{-1}$  in the spectrum of 1,3-dimethylurea to the amide I mode.<sup>59</sup> Iijima et al.<sup>60</sup> have pointed out the presence of a single amide I band at  $1650\text{ cm}^{-1}$  in the spectrum of polyurea. Skrovanek et al.<sup>61</sup> have associated the intense band at  $1640\text{ cm}^{-1}$  and the shoulder at about  $1670\text{ cm}^{-1}$  observed in the spectra of amorphous polyamides with hydrogen-bonded and “free” carbonyl groups, respectively. Zharkov et al.<sup>66</sup> have recently investigated in detail the amide I absorption band contour of the infrared spectra of polyether urethane elastomers and have concluded that it comprises five individual components at  $1740$ ,  $1730$ ,  $1725$ ,  $1713$ , and  $1702\text{ cm}^{-1}$ . Several associations for the urethane groups have been proposed to account for the isolated bands observed. Coleman et al.<sup>62</sup> have reported the presence of three bands in the carbonyl stretching region of a simple polyurethane, at about  $1721$ ,  $1699$ , and  $1684\text{ cm}^{-1}$ , which have been assigned to non-hydrogen-bonded and disordered and ordered hydrogen-bonded C=O groups, respectively. In model polyurethanes two clearly discernible components have been found in the amide I region: one at  $1732\text{ cm}^{-1}$ , assignable to carbonyls free of hydrogen bonding, and another at  $1703\text{ cm}^{-1}$ , associated with hydrogen-bonded carbonyls.<sup>63</sup> In urethane–ether blends two components have also been found in this range of frequencies: the free carbonyl band at  $1725\text{ cm}^{-1}$  and the hydrogen-bonded carbonyl band located between  $1694$  and  $1704\text{ cm}^{-1}$ .<sup>65</sup>

It may be immediately inferred from Figure 4 that the amide I region in the ureasils is extremely complex. This is not surprising considering that the urea moiety contains two N–H groups, whereas in polyamides and polyurethanes only one N–H group contributes to hydrogen bonding. Moreover, in the ureasils, as pointed out above, the two N–H groups of the urea cross-link are expected to behave differently, since one of them is bonded to a propyl chain, which is in turn bonded to a rigid silicon-based network, whereas the other is bonded to soft organic oxy(ethylene) chains.

In the spectrum of U(600) the amide I mode gives rise to a very intense broad band whose maximum occurs at  $1643\text{ cm}^{-1}$  (Figure 4a). The maximum of the band is upshifted to  $1751\text{ cm}^{-1}$  in the spectrum of U(2000) (Figure 4c). The amide I region of U(900) (Figure 4b) spans a larger range of frequencies than the previous

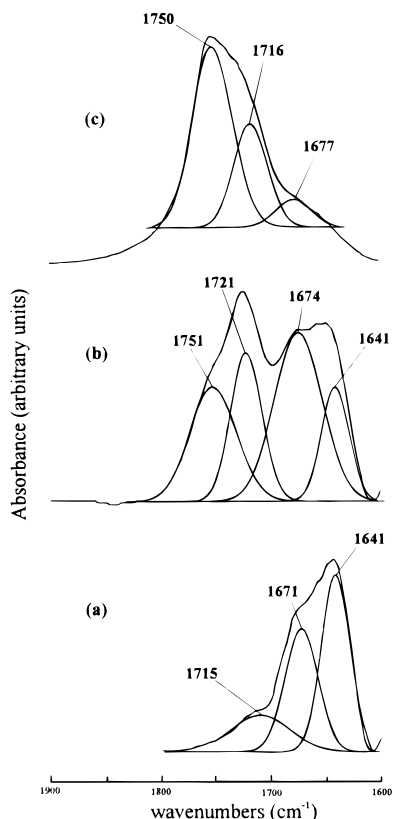


**Figure 5.** Curve-fitting results of the room-temperature amide I region of the undoped ureasils: (a) U(600), (b) U(900), and (c) U(2000).

materials, since two strong broad envelopes centered at about 1724 and 1650  $\text{cm}^{-1}$  are now observed. Two immediate conclusions may be drawn from the analysis of these results. (1) The spectral feature of the amide I band of these hybrid materials is drastically modified as the length of the oxy(ethylene) chains present is increased from 8.5 in U(600) to about 40.5 in U(2000). (2) The spectra of the ureasils in the range 1600–1800  $\text{cm}^{-1}$  provide conclusive evidence that several components contribute to the envelope of the amide I band, meaning that various more or less ordered structures involving hydrogen bonding between the N–H groups of urea and the oxygen atoms of ether or carbonyl moieties are possible.

To determine the frequency of these components, we have performed curve-fitting of the bands with the ORIGIN computer software for IBM PC-compatible computers. Gaussian bands shapes were employed in this procedure, since they produced the best fits. A linear baseline was assumed in the three cases from 2000 to 400  $\text{cm}^{-1}$  for the points where no significant absorbances were detected. Curve-fitting was limited to the 1760–1610 and 1830–1610  $\text{cm}^{-1}$  spectral ranges in the case of U(600) and U(900), respectively; for U(2000) the limits were set between 1805 and 1640  $\text{cm}^{-1}$ . A minimum of three components was isolated for the amide I band of U(600) at 1715, 1671, and 1641  $\text{cm}^{-1}$  (Figure 5a). The amide I spectral region of U(900) was resolved into four components at 1751, 1721, 1674, and 1641  $\text{cm}^{-1}$  (Figure 5b). At last, three individual components were detected for U(2000) at 1750, 1716, and 1677  $\text{cm}^{-1}$  (Figure 5c). Thus, four components—centered around 1751, 1721, 1674, and 1641  $\text{cm}^{-1}$ —seem to

describe entirely the amide I region of the three hybrid compounds.

However, these results should be looked at with extreme care. First of all, the second-derivative absorbance spectra (smoothed by a cubic function by averaging 10 points) were not always consistent with the deconvolution procedure. Only in the case of U(900) did the frequency of the bands match exactly that indicated by the second-derivative plot. Second, the fitting procedure is subject to much ambiguity, since it depends heavily on the baseline drawn, on the band frequency limits set initially, and on the number and position of the bands. Third, the breadth of the components was totally unknown and could not be estimated previously. Considering all these items, the results just described might be physically meaningless. An alternative approach within a statistic framework will be considered in the near future to confirm them.

**Bands in the Amide II Region.** The amide II mode is a mixed contribution of the N–H in-plane bending, the C–N stretching, and the C–C stretching vibrations.<sup>68</sup> It is sensitive to both chain conformation and intermolecular hydrogen bonding. In noncyclic secondary amides, where the N–H and C=O groups exist mainly in a trans configuration, the in-plane N–H bending frequency and the resonance-stiffened C–N bond stretching frequency fall close together and interact considerably, giving rise to a strong absorption near 1550  $\text{cm}^{-1}$ .<sup>68,70</sup>

The amide II band is seen at 1545  $\text{cm}^{-1}$  in amorphous polyamides<sup>61</sup> and at 1540  $\text{cm}^{-1}$  in simple polyurethanes.<sup>62</sup> In disubstituted ureas bands, bands in the 1510–1560<sup>58</sup> and 1565–1590  $\text{cm}^{-1}$ <sup>59</sup> spectral regions have been ascribed to the amide II mode. In the spectra of the *N,N*-disubstituted ureas studied by Mido,<sup>55</sup> the amide II band is located between 1565 and 1590  $\text{cm}^{-1}$ . Nevertheless, this author has noted that the amide II band of derivatives having branched alkyl groups appear at slightly lower frequencies. Therefore, we associate the single intense band seen at 1565  $\text{cm}^{-1}$  in the spectra of U(600) (Figure 4a) and U(900) (Figure 4b) with this vibration mode. This assignment is corroborated by the fact that the amide II band of 1-ethyl-3-*tert*-butylurea has been found at exactly this frequency.<sup>55</sup> The band is downshifted to 1548  $\text{cm}^{-1}$  in the spectrum of U(2000), and its intensity is markedly reduced (Figure 4c). The polyurea thin films investigated by Iijima et al.<sup>60</sup> display this band at 1550  $\text{cm}^{-1}$ . Person et al.<sup>75</sup> have demonstrated that the reduction in frequency and intensity of this mode may be correlated with a decrease in hydrogen-bonding strength. This would imply that the hydrogen bonds in U(2000) are less strong than in the other two ureasils considered. It is interesting to mention the interpretation given by Myers to account for the changes observed in the 1510–1560  $\text{cm}^{-1}$  spectral region of urea–formaldehyde polymers during curing.<sup>58</sup> He has reported the presence of a strong amide II band in the spectra of uncured polymers between 1550 and 1560  $\text{cm}^{-1}$  and the appearance and growth of a band at 1510–1520  $\text{cm}^{-1}$  during polymer cure. According to this author, although in the uncured solid form the material must exist primarily as a linear chain in a highly hydrogen-bonded state,

(75) Person, W. B.; Zerbi, G. *Vibrational Intensities in Infrared and Raman Spectroscopy*; Elsevier: Amsterdam, 1982.

after curing hydrogen bonding is possibly repressed because of steric constraints.

**Bands in the Amide III Region.** The amide III mode involves the stretching vibration of the C–N group. It is highly mixed and complicated by coupling with NH deformation modes. The amide III band is expected between 1250 and 1350  $\text{cm}^{-1}$ .<sup>68</sup>

Urea–formaldehyde resins are known to absorb broadly at 1260 and 1290  $\text{cm}^{-1}$  because of this vibration mode prior to and after curing, respectively.<sup>58</sup> A strong and broad amide III band has been observed between 1260 and 1300  $\text{cm}^{-1}$  in the spectra of the resins prepared by Jada.<sup>59</sup> The frequency of this band in the spectrum of polyurea has not been reported.<sup>60</sup> In the spectrum of dialkylureas this band appears in the 1240–1330  $\text{cm}^{-1}$  region.<sup>55</sup> We therefore ascribe the medium-intensity band observed at 1276  $\text{cm}^{-1}$  in the spectrum of U(600) (Figure 4a) and at 1284  $\text{cm}^{-1}$  in both the spectra of U(900) (Figure 4b) and U(2000) (Figure 4c) to this mode. This assignment is supported by the following evidence. (1) In 1-*n*-butyl-3-*sec*-butylurea and in 1-*sec*-butyl-3-*sec*-butylurea the amide III mode gives rise to an intense absorption band at 1275  $\text{cm}^{-1}$ .<sup>55</sup> The band at 1276  $\text{cm}^{-1}$  in the spectrum of 1-ethyl-3-*sec*-butylurea has also been attributed to this vibration.<sup>55</sup> (2) 1-Methyl-3-*tert*-butylurea and 1-*n*-butyl-3-butylurea display the amide III band at 1282 and 1286  $\text{cm}^{-1}$ , respectively.<sup>55</sup>

**Bands in the Amide IV, V, and VI Regions.** The amide IV, V, and VI bands are produced by highly mixed modes containing a significant contribution from the NH out-of-plane deformation mode. They are expected to be in the 800–400  $\text{cm}^{-1}$  region.<sup>55</sup>

Owing to the influence of the alkyl framework on its strength, the amide IV band is often absent in the spectra of urea derivatives. For instance, Mido<sup>55</sup> has been unable to detect it experimentally in any of the spectra of the 30 dialkylureas he analyzed.

The amide V vibration mode absorbs strongly and broadly in the 630–690  $\text{cm}^{-1}$  region.<sup>55,68</sup> Although the *N,N*-disubstituted ureas investigated by Mido exhibit this band at frequencies lower than 672  $\text{cm}^{-1}$ ,<sup>55</sup> we tentatively assign the weak-to-very-weak band observed at 692  $\text{cm}^{-1}$  in the spectra of U(600) and U(900) (Figures 4a and 4b, respectively) and at 698  $\text{cm}^{-1}$  in the spectrum of U(2000) (Figure 4c) to this mode.

Taking into account that in the spectra of disubstituted urea derivatives the amide VI band has been reported to appear constantly ca. 770  $\text{cm}^{-1}$ ,<sup>55</sup> we attribute the very weak bands observed at 775, 771, and 761  $\text{cm}^{-1}$  in the spectra of U(600), U(900), and U(2000), respectively, to the amide VI mode.

At last, a medium-intensity band over the region between 600 and 500  $\text{cm}^{-1}$  observed in the spectra of disubstituted ureas has been attributed to  $\delta(\text{N}-\text{C}-\text{N})$  by analogy to the case of methylalkylureas.<sup>55</sup> Considering that the very weak bands at 669 and 638  $\text{cm}^{-1}$  found respectively in the spectra of U(600) and U(2000) are not observed in the spectra of the parent diamines (see Tables 1 and 2), we tentatively assign them to this mode.

Let us now go back to the interpretation of the room-temperature amide I and II bands of the ureasils. The discussion that follows shows that the present spectroscopic work has helped to clarify several points related

to the structure of the materials. It is based on two important assumptions. (1) Because of the hybrid nature of the ureasils, the N–H groups of the urea moieties are expected to behave differently. (2) The amide I bands of U(600), U(900), and U(2000) are definitely decomposed into three, four, and three components, respectively, as suggested by the curve-fitting procedure described earlier.

The mid-infrared spectrum of U(600), in particular the location of the amide I band, indicates that the interaction between the N–H groups and the oxygen atoms of the C=O or OCH<sub>2</sub>CH<sub>2</sub> groups is apparently sterically favorable for the formation of strong and ordered hydrogen-bonded structures. This particular behavior may be associated with the intrinsic nature of the material. Since U(600) contains fewer oxyethylene units than the other ureasils, the number of urea moieties present is extremely high. Hence, self-association of the latter group is expected to occur extensively throughout the material. This situation is aided by the flexibility of the chaotically distributed oligopolyether segments that are able to adopt easily adequate spatial conformations for highly efficient hydrogen bonding.

In semicrystalline U(2000) the opposite situation takes place. The remarkable upshift of the amide I band (108  $\text{cm}^{-1}$ ) of U(600) upon incorporation of 32 more oxyethylene units is accompanied by a marked decrease of the intensity of the amide II band. Judging from these results, we may state that the associations formed in U(2000) via hydrogen bonds must be considerably weaker than those in U(600). The steric constraints created by the extra repeat units very possibly account for this behavior. Because of the considerable number of oxyethylene units present, the influence of the urea linkages in this ureasil is minimized and the formation of hydrogen-bonded urea–polyether associations favored. On the basis of the premise that whenever hydrogen bonding occurs between a urea moiety and one ether oxygen of a soft polyether segment one carbonyl group is liberated, a large number of “free” carbonyl groups is expected to exist in U(2000).

The proportion of hydrogen-bonded urea–polyether and urea–urea associations in the three ureasils helps to explain the number and intensity of the components observed in the amide I spectral region of the corresponding spectra.

The contour of the amide I band in the spectrum of U(2000) (Figure 5c) shows that the most intense component is situated at 1750  $\text{cm}^{-1}$ . Considering its extremely high frequency, we tentatively assign it to the absorption of urea groups completely devoid of any hydrogen bonding (either by N–H or by C=O groups). We attribute the remaining two components at 1716 and 1677  $\text{cm}^{-1}$  to the vibration of NHC(=O)NH groups belonging to urea–polyether structures, which will be designated as A and B, respectively. The amide I region of semicrystalline nylon is also composed by three bands that have been attributed to hydrogen-bonded carbonyl groups in ordered domains, hydrogen-bonded carbonyl groups in disordered conformations, and “free” carbonyl groups.<sup>61</sup> Since the bands at approximately 1716 and 1677  $\text{cm}^{-1}$  are present in the three ureasils studied, we cannot associate them unequivocally with amorphous or crystalline domains.



In U(600), ordered self-associated urea–urea structures C dominate, giving rise to the strong component at  $1641\text{ cm}^{-1}$  (Figure 5a). Since the band at  $1641\text{ cm}^{-1}$  is missing in the spectrum of U(2000), we are led to conclude that no urea–urea hydrogen-bonded associations are present in the latter ureasil. On the other hand, the absence of an individual band at  $1750\text{ cm}^{-1}$  in the spectrum of U(600) is an indication that the extension of hydrogen bonding throughout this material is such that neither C=O nor N–H groups are left free. This claim is acceptable considering the length of the polyether chains in both materials; there are approximately 5 times more (OCH<sub>2</sub>CH<sub>2</sub>) units in U(2000) than in U(600). The other components of the amide I absorption band of U(600) at  $1671$  and  $1715\text{ cm}^{-1}$  are inherent to progressively less ordered urea–polyether structures B and A, respectively. The prominence of hydrogen bonding in U(600), caused by the presence of urea groups, is not unexpected at all. Quite recently, similar interactions have allowed De Loos et al.<sup>76</sup> and van Esch et al.<sup>77</sup> to synthesize new durable organic gels with potential applications through self-assembly and polymerization. Highly specific interactions between neighboring urea groups of a bis-ureido derivative provide excellent gelling properties to this compound. When added to common solvents, elongated fibers are formed via hydrogen bonding.

The spectrum of U(900) exhibits a more complicated amide I band contour (Figure 5b), suggesting definitely a situation between that found in the spectra of the higher and lower analogues. Probably short and long N–H···O contacts are established, for the length of the soft segments and the number of urea moieties are such that the N–H groups of the urea linkage may now interact indiscriminately with the carbonyl and the

ether oxygen atoms of the soft polyether segments. The component of the amide I absorption band of U(900) centered at  $1641\text{ cm}^{-1}$  (Figure 5b) indicates that though the formation of the urea–polyether structures B and A is preferred, that of urea–urea associations (structure A) is also feasible. The presence of the band at  $1751\text{ cm}^{-1}$  proves that “free” C=O groups exist too.

It is worth mentioning that the relative breadth of the bands in the three compounds gives some confidence to the curve-fitting procedure. The infrared band attributed to urea–urea interactions at  $1641\text{ cm}^{-1}$  is, as expected, considerably narrower than those of the other components. Its width at half-height has the same magnitude for U(600) and U(900) ( $W_{1/2} = 24\text{ cm}^{-1}$ ). The width at half-height of the band at  $1750\text{ cm}^{-1}$ , associated with “free” carbonyl groups, is larger and has a similar value for U(2000) and U(900) ( $W_{1/2} = 37$  and  $42\text{ cm}^{-1}$ , respectively). The width at half-height of the band situated at approximately  $1674\text{ cm}^{-1}$ , associated with structure B, is  $37$ ,  $43$ , and  $31\text{ cm}^{-1}$ , respectively, for U(600), U(900), and U(2000). Finally, the band at about  $1716\text{ cm}^{-1}$ , attributed to the hydrogen-bonded structure A, has a width at half-height of  $40$ ,  $28$ , and  $30\text{ cm}^{-1}$ , respectively, for U(600), U(900), and U(2000).

The temperature-dependent spectral studies of the ureasils that will be performed in the near future will hopefully provide valuable and enlightening information about the rich spectral feature of these fascinating materials.

**Acknowledgment.** The authors thank Dr. A. M. Amorim da Costa, of the Department of Chemistry of the University of Coimbra, and Dr. Ivone Delgadillo, of the Department of Chemistry of the University of Aveiro, for helpful discussions. The financial support of Fundação para a Ciência e Tecnologia (contract number PBIC/CTM/1965/95) is greatly appreciated.

CM980372V

(76) De Loos, M.; van Esch, J.; Stokroos, I.; Kellogg, R. M.; Feringa, B. L. *J. Am. Chem. Soc.* **1997**, *119*, 12675.

(77) van Esch, J.; Kellogg, R. M.; Feringa, B. L. *Tetrahedron Lett.* **1997**, *38* (2), 281.